LA-UR-21-21776

Title:	(U) Recalculation of Soil Bulk Density Used in the Scorpius MCNP6 Model
Author(s):	Favorite, Jeffrey A.
Intended for:	Report
Issued:	2021-02-23

Los Alamos
NATIONAL LABORATORY
memorandum
X-Computational Physics Division
Radiation Transport Applications Group
Group XCP-7, MS F663
Los Alamos, New Mexico 87545
505/667-1920

To/MS: Distribution
From/MS: Jeffrey A. Favorite / XCP-7, MS F663
Phone/Email: 7-7941 / fave@lanl.gov
Symbol: XCP-7:21–007(U) (LA–UR–21–?????)
Date: February 22, 2021

SUBJECT: (U) Recalculation of Soil Bulk Density Used in the Scorpius MCNP6 Model

I. Introduction

The soil composition used in the Scorpius MCNP6.2 (Ref. 1) model was recently recalculated.[2] Originally, it was "determined using the United States Geological Survey (USGS) Mercury Core Library and the Nevada National Security Site U.S. Geological Survey Databases (NNSS USGS) and Nevada National Security Site Petrographic, Geochemical, and Geophysical Database (NNSS PGG)," [3,4] but the details had been lost. Reference 2 documents the updated soil composition determination.

Reference 2 estimated the grain density of the soil instead of the bulk density. This report corrects that error. I am indebted to Garrett Euler (EES-17) for reading Ref. 2, pointing out its errors, and guiding me through the correct calculations.

This report is organized as follows. For completeness, the composition calculations from Ref. 2 are repeated: Sec. II discusses the data that are reported in the PGG Access database, and Sec. III uses the data in the PGG Access database to compute the composition of the soil. Section IV estimates the bulk density of the soil. Section V evaluates the soil wall thickness in the Scorpius model. Section VI estimates the effect of the soil density change on previously calculated results. Section VII presents a summary and conclusions. Input files and output files are listed in appendices.

II. Data in the PGG Access Database

The NNSS PGG Database is a MicroSoft Access file available from the Mercury Core Library and Data Center.[5] "NNSS PGG Database" is under "Archival Data" on the left of the page; a direct link is given in Ref. 6. The database file itself is a Windows zip file.[7] Supposedly, the data is "published and documented in USGS Data Series Report 297,"[8] but I could not determine where Report 297[8] discussed compositions or oxides.

A MicroSoft Excel spreadsheet[9] obtained from Tim Goorley (XCP-7) was very helpful in guiding me to the appropriate tables in the PGG Access database. The Access file is enormous and there may be relevant data that were missed.

In the database,[7] table "tbl_ca_measure" includes the data shown in Table I with the label "spl_id" equal to "U1A01/F767/13.1(A". In addition to the data shown in Table I, each entry has label "Strat Code" equal to "Tyo", label "Sam_Type Code" equal to "T", label "Lith Code" equal to "BED", label "Altn" equal to "GL/CC", and labels "ref_code" and "mAlt" blank.

Table "dsc_units_list" says that units code P has name "ppm" and description "parts per million" and code T has name "tot %" and description "total percent." These relative units are conventionally given on a mass basis.[10] In this report, a mass basis is assumed. It is always a good idea to be explicit about this.

Table I. Composition Data from the NNSS PGG Access Database.

oxide_code	oxide_value	oxide_error	oxide_error_ meth_code	oxide _ldl	units_ code	ca_subtype_ code	n_rep	entry_date
Al2O3	11.24	0.27	M		T	RH	1	23-Oct-1998
BaO	515.7	32	M		P	RH	2	23-Oct-1998
CaO	3.155	0.093	M		T	RH	2	23-Oct-1998
Cr2O3				11.86	P	RH	2	23-Oct-1998
Fe2O3	1.351	0.057	M		T	RH	1	23-Oct-1998
K2O	5.838	0.057	M		T	RH	1	23-Oct-1998
MgO	0.1911	0.074	M		T	RH	2	23-Oct-1998
MnO	0.03027	0.01	M		T	RH	2	23-Oct-1998
Na2O	2.007	0.089	M		T	RH	1	23-Oct-1998
Nb2O5	77.79	8.2	M		P	RH	2	23-Oct-1998
NiO	8.272	7.4	M		P	RH	2	23-Oct-1998
P2O5	0.01408	0.012	M		T	RH	2	23-Oct-1998
Rb2O	185.1	6	M		P	RH	2	23-Oct-1998
SiO2	68.02	0.89	M		T	RH	1	23-Oct-1998
SrO	36.47	5.8	M		P	RH	2	23-Oct-1998
TiO2	0.1198	0.014	M		T	RH	2	23-Oct-1998
V2O3				10.17	P	RH	2	23-Oct-1998
Y2O3	91.29	7.3	M		P	RH	2	23-Oct-1998
ZnO	75.89	39	M		P	RH	2	23-Oct-1998
ZrO2	227.3	16	M		P	RH	2	23-Oct-1998
LOI	6.48				T		1	25-Mar-2003
Total	98.45				T	RH	2	23-Oct-1998

It should be noted that the "Total" given in the database is not correct. It was evidently obtained by dividing the ppm values by 10^6 and adding them to the sum of the percent values. This procedure mixes units. The correct total is obtained by dividing the ppm values by 10^6 and then multiplying them by 100, which puts them in percent, and then adding them to the sum of the percent values. The correct total is 98.57 wt%, where, as mentioned earlier in this section, a mass basis is assumed.

The uncertainty of the sum (assuming the values in "oxide_error" are uncorrelated) is 0.9455 percentage points or about 1% of the total of 98.57 wt%. So a total of 100% is about 1.5σ away from the actual total.

Two of the oxides, Cr_2O_3 and V_2O_3, were not detected. Their lowest detectable limits are listed in Table I.

III. Determining the Soil Composition

As before,[3,4] it was assumed that the material lost on ignition (LOI) was pure water. The two oxides not detected were ignored in this analysis.

The Elementary module[11] of Faust was used to determine the isotopic composition of each oxide based on pure stoichiometry. Isotopic abundance data from Ref. 12 were used. The input and output for Elementary are listed in Appendix A. The input and output are both on an atom basis.

MCNP6.2 was used to convert the stoichiometric compositions, including all isotopes, from an atom basis to mass fractions. The Elementary output was used in an MCNP6.2 input file that had one material for each oxide. The input file and the output of interest, print table 40, are listed in Appendix A.

The isotopic mass fractions of the oxide components were then multiplied by the "oxide value" (oxide composition by weight) listed in Table I, dividing by 100 or 10^6, as appropriate. Finally, as before,[3,4] the results were normalized to sum to unity.

The final composition is listed in Table II.

Table II. Soil Composition, Normalized.[(a)]

ZAID	Wgt. Frac.	ZAID	Wgt. Frac.	ZAID	Wgt. Frac.	ZAID	Wgt. Frac.
1001	7.35469E-03	20040	2.21124E-02	28058	4.43139E-06	39089	7.29297E-05
1002	1.69047E-06	20042	1.54953E-04	28060	1.76576E-06	40090	8.65648E-05
8016	5.08370E-01	20043	3.31024E-05	28061	7.80371E-08	40091	1.90879E-05
8017	2.05809E-04	20044	5.23362E-04	28062	2.52889E-07	40092	2.94970E-05
8018	1.17560E-03	20046	1.04919E-06	28064	6.64830E-08	40094	3.05435E-05
11023	1.51054E-02	20048	5.11833E-05	30064	2.94072E-05	40096	5.02560E-06
12024	9.11348E-04	22046	5.76933E-05	30066	1.73985E-05	41093	5.51686E-05
12025	1.20189E-04	22047	5.31601E-05	30067	2.59559E-06	56130	4.69873E-07
12026	1.37607E-04	22048	5.37918E-04	30068	1.20470E-05	56132	4.54598E-07
13027	6.03520E-02	22049	4.02988E-05	30070	4.10088E-07	56134	1.10437E-05
14028	2.96354E-01	22050	3.93714E-05	37085	1.23122E-04	56135	3.03453E-05
14029	1.55858E-02	25055	2.37834E-04	37087	4.85947E-05	56136	3.64225E-05
14030	1.06279E-02	26054	5.41213E-04	38084	1.67800E-07	56137	5.24714E-05
15031	6.23408E-05	26056	8.81016E-03	38086	3.02475E-06	56138	3.37390E-04
19039	4.56954E-02	26057	2.07104E-04	38087	2.17237E-06		
19040	5.88004E-06	26058	2.80448E-05	38088	2.59217E-05		
19041	3.46683E-03						

(a) The sum of the entries is 1.00000.

IV. Mass Density of Soil

Reference 3 contains this explanation of the determination of the current soil mass density: "The density of the tuff was calculated by multiplying the oxide fraction (as calculated from the percent of total) by their researched density and summing across all 20 oxides for the total value, which came to 2.695 g/cm^3." The "researched density" is presumably a handbook density. Handbook densities for the detected oxides of Table I are shown in Table III.

Table III. Handbook Oxide Densities.[13]

Oxide	Density (g/cm^3)
Al_2O_3	3.99, 3.97
BaO	5.72
CaO	3.34
Fe_2O_3	5.25
K_2O	2.35
MgO	3.6
MnO	5.37
Na_2O	2.27
Nb_2O_5	4.47
NiO	6.72
P_2O_5	2.30
Rb_2O	4.0
SiO_2	2.648, 2.533, 2.265, 2.334, 2.196
SrO	5.1
TiO_2	3.9
Y_2O_3	5.03
ZnO	5.6
ZrO_2	5.68

Multiplying the densities of Table III by the "oxide values" of Table I (using the first entry listed for Al_2O_3 and SiO_2) and summing yields a grain density of 2.629 g/cm^3, 2.4% less than the 2.693 g/cm^3 reported in Ref. 2. This calculation does not include the 6.48% LOI in Table I that was assumed to be water. In Ref. 2, water was incorrectly included. Again, this calculation yields an estimate of the grain density, not the bulk density needed for transport calculations.

Allen (Ref. 14, Table 8) gives an average grain density for U-1a.01 and U-1a.02 as 2.609 g/cm^3. The value computed above (2.629 g/cm^3) is only 0.8% larger. The different SiO_2 densities in Table III give the grain densities shown in Table IV. Based on Allen's reported average grain density, the largest SiO_2 density seems to be the most likely value.

Table IV. Grain Density as a Function of SiO_2 Density.

SiO_2 Density (g/cm^3)	Grain Density (g/cm^3)
2.648	2.629
2.533	2.550
2.334	2.415
2.265	2.368
2.196	2.321

Reference 2 reported the grain density instead of the bulk density. (All Scorpius calculations up to now have used some estimate of the soil grain density instead of the soil bulk density.) We now estimate the bulk density of the soil.

The volume fraction porosity ϕ is related to the bulk density ρ_0, the grain density ρ_g, and the weight fraction W of water in the rock according to[15]

$$\phi = 1 - \frac{\rho_0(1-W)}{\rho_g}. \tag{1}$$

Rearranging Eq. (1) gives the bulk density as

$$\rho_0 = \frac{\rho_g(1-\phi)}{1-W}. \tag{2}$$

Allen (Ref. 14, p. 39) gives the porosity as 25% to 36% (these are calculated, not measured). Allen (Ref. 14, p. 45) gives the measured water content from the LYNER (Low Yield Nuclear Explosive Research) complex as 2.4% to 12.9%. (The value of 6.48% inferred from Table I is consistent with this range.) We assumed the grain density varies from 2.609 g/cm^3 (Ref. 14, Table 8) to 2.629 g/cm^3 (calculated above).

These parameters were sampled independently and uniformly, with bounds given in Table V, one million times. The bulk density was computed using Eq. (2) for each realization. The resulting distribution of the bulk density is shown in Figure 1. It is approximately a Gaussian centered at 1.96 g/cm^3 with half-width 0.12 g/cm^3. The bulk density of the soil according to this analysis is thus 1.96 g/cm^3 ± 6%. The uncertainty is probably underestimated.

Table V. Parameters Sampled for Bulk Density Distribution.

Parameter	Minimum	Maximum
Grain density, ρ_g	2.609 g/cm^3	2.629 g/cm^3
Water fraction, W	2.4%	12.9%
Porosity, ϕ	25%	36%

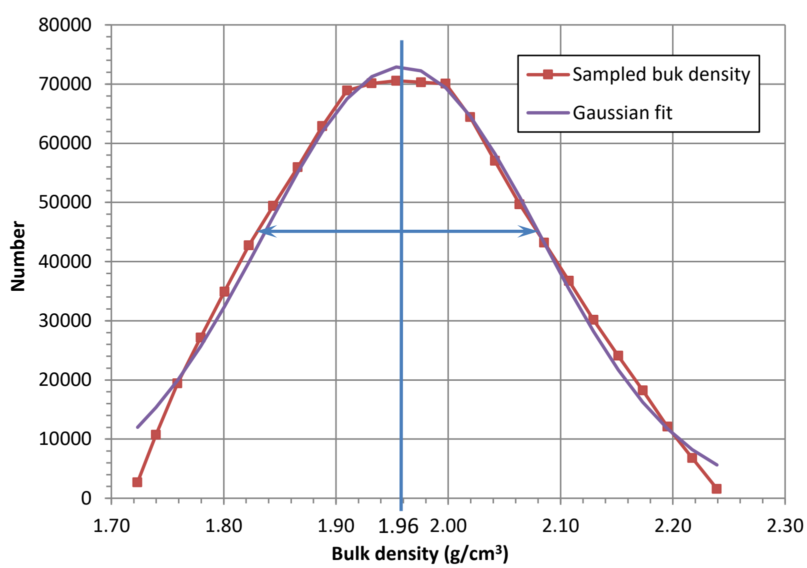

Figure 1. Bulk density distribution.

V. Soil Thickness Needed in the Model

The minimum soil wall thickness in the Scorpius model[4] seems to be 152.4 cm. I do not know how that thickness was determined, and I have always wondered if it is thick enough. With the bulk density of the soil in the model reduced by 27%, in this section we reconsider the soil thickness.

Calculations were done with MCNP6.2.1.1. We used the simplified model of the U1a 100 Drift shown in Figure 2. The thickness of the wall is 152.4 cm. A gamma-ray beam was directed normal to the wall from a point source 119.52 cm above the floor, 2.54 cm from the wall, and centered along the length of the tunnel, as shown in Figure 2. The gamma-ray source had discrete energies of 1, 2, 3, 4, 5, 6, 7, 8, 9, 10, 11, 12, 13, 14, and 15 MeV, all uniformly sampled. The neutron and gamma-ray currents emerging from the wall back into the drift were tallied as a function of the source gamma-ray energy. If thickening the soil wall changes the emitted current, then the soil wall is not thick enough.

The soil wall thickness was increased by 100, 200, 300, and 400 cm by moving the outer surface away from the drift. The wall thickness was also decreased by 130 cm by moving the outer surface towards the drift. The input file for the nominal case is listed in Appendix B.

Results are shown Figure 3. Thickening the soil wall has no effect on the neutron or gamma-ray emission into the drift. The soil wall was thinned to see if there was any effect at all, and there is. We conclude that the soil wall thickness in the Scorpius model is sufficient, even with the reduced soil density.

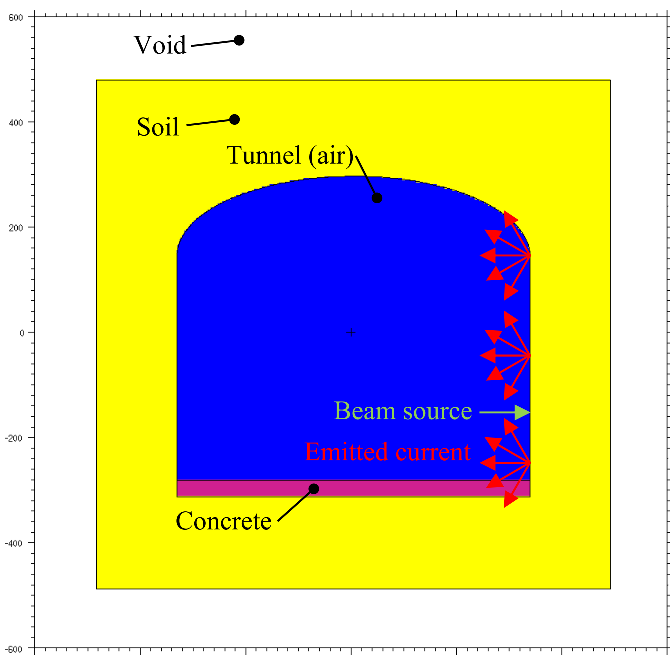

(a)

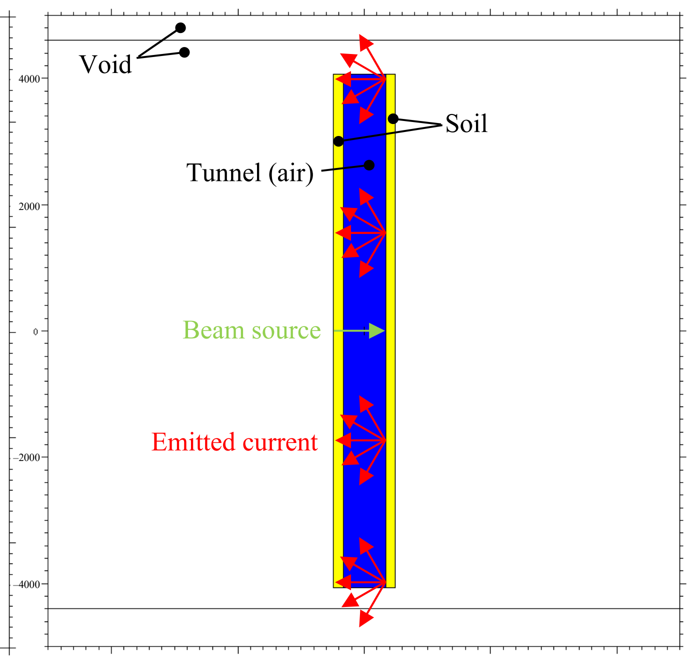

(b)

Figure 2. 100 Drift model. (a) Cross section of tunnel. (b) Plan view. The beam source is located correctly except that it is 1 inch from the wall. The red arrows show where the current is tallied and its direction into the tunnel (the arrows are not meant to suggest the actual angular or spatial distribution). Scales in centimeters.

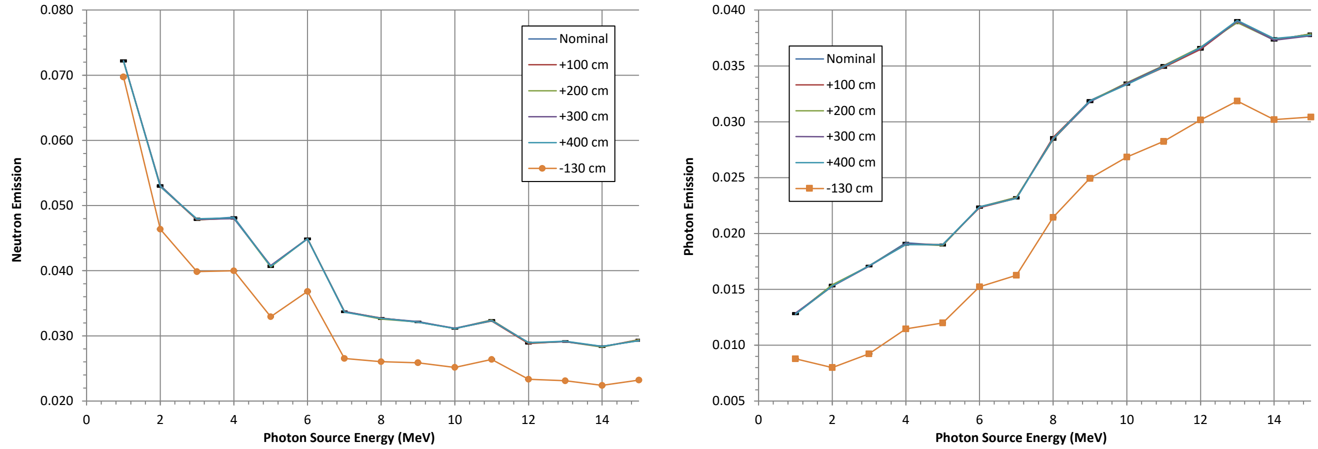

(a) (b)

Figure 3. Neutron and photon emission as a function of gamma-ray source energy and soil wall thickness. 1σ statistical uncertainties are shown. The curves are statistically identical except for "-130 cm".

VI. Effect of Soil Density Change

VI.A. Beam Normal to the Wall

The effect of the soil density decrease of 27% was estimated using the same model presented in Sec. V. In this case the soil wall thickness stayed constant (at its nominal value), but the density was varied. Results are shown in Figure 4. Decreasing the density to the new nominal value has no effect on the neutron or gamma-ray emission into the drift. Even decreasing the density all the way down to 0.5 g/cm^3 (a 74.5% decrease from the new nominal density of 1.96 g/cm^3) decreases the neutron emission by 4.2% and the gamma-ray emission by 9.9% (integrated over energy).

The emission in this test is not very sensitive to the soil density.

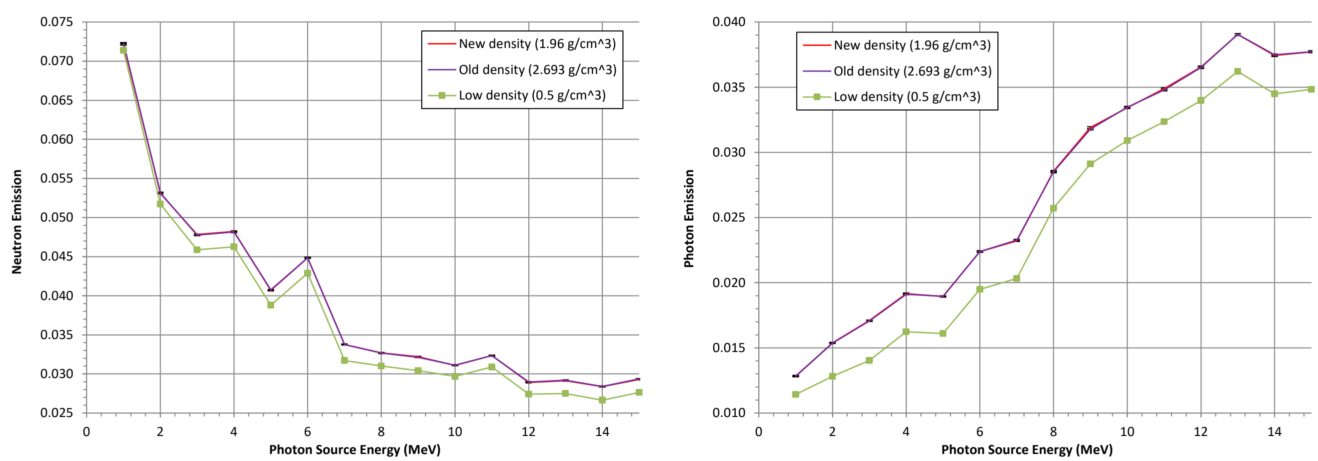

(a) (b)

Figure 4. Neutron and photon emission as a function of gamma-ray source energy and soil density. 1σ statistical uncertainties are shown. The curves are statistically identical except for "Low density".

VI.B. Beam Approximately Parallel to the Wall

Radiation will travel further through the soil parallel to the drift when the soil density is decreased in the calculations. The calculation of Ref. 16 has been redone with the new density. Results are shown in Figure 5. The difference between the results of Figure 5 and those of Ref. 16, defined as

$$\text{difference} = \frac{J(1.96) - J(2.693)}{J(2.693)}, \tag{3}$$

where J is the current, are shown in Figure 6. The neutron currents vary by about 20%, but there is no trend and the uncertainty in the difference is generally greater than the difference, except at the smallest and largest energies. The photon currents vary by less than 2%, except and the smallest energies, and there is a clear trend: The photon current entering the 100 Drift is about 2% larger (at higher energies) with the smaller soil density. There does not seem to be a trend in the photon current entering Plug A, however.

Based on the results of this section, it is estimated that the change in density probably does not significantly affect the calculations reported in the 60% Plug B shielding design report.[3]

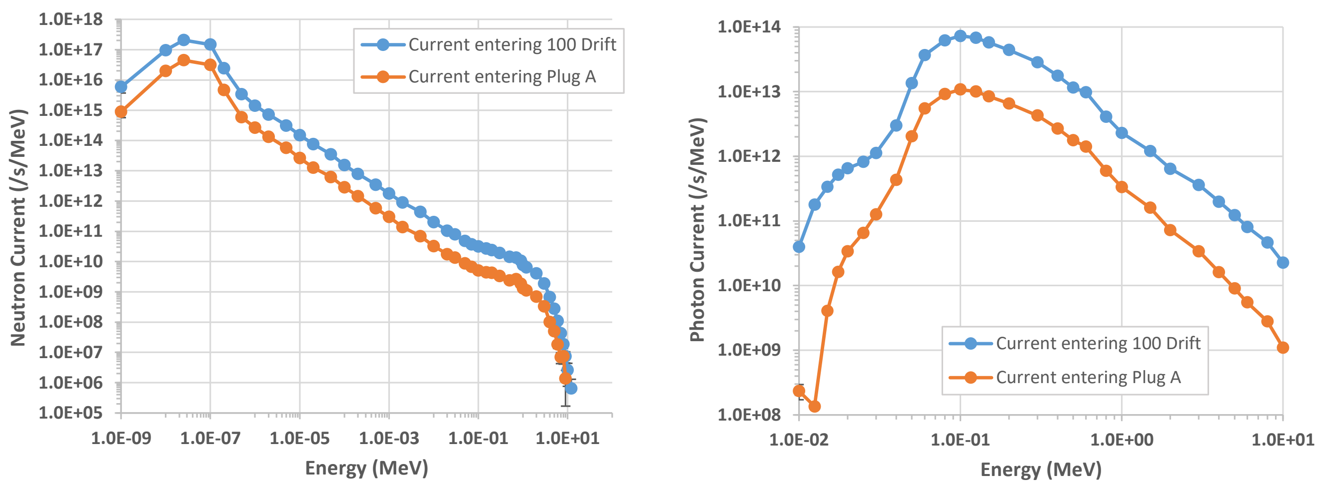

(a) (b)

Figure 5. (a) Neutron and (b) photon currents entering the 100 Drift and Plug A. The new soil density (1.96 g/cm^3) is used. 1σ statistical uncertainties are shown.

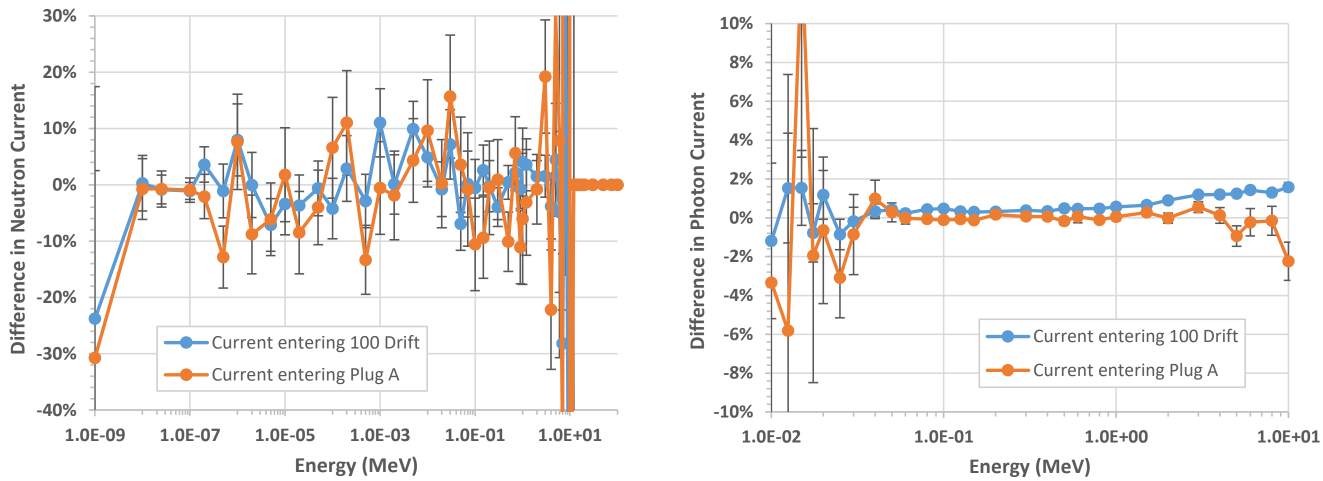

(a) (b)

Figure 6. Difference between (a) neutron and (b) photon currents of Ref. 16 and currents of Figure 5 (relative to currents of Ref. 16). 1σ statistical uncertainties are shown.

VII. Summary and Conclusions

The U1a soil composition for Scorpius was updated in Ref. 2, but the density calculated there was incorrect. This report estimates the bulk density of the soil as 1.96 g/cm^3 ± 6%. The uncertainty is underestimated, but a better estimate is not available.

The long-standing use of the incorrect soil density probably does not affect previously reported results, particularly those in the 60% Plug B shielding design report.[3] However, if the old soil model has been used to compute dose rates from activated soil, those results are probably incorrect.

The description of the soil composition and density calculation should be modified in the Scorpius input file and in any future documentation. Here is the new description:

> The U1a soil composition was determined using the United States Geological Survey (USGS) Mercury Core Library and the Nevada National Security Site U.S. Geological Survey Databases (NNSS USGS) and Nevada National Security Site Petrographic, Geochemical, and Geophysical Database (NNSS PGG). The composition of the soil is important as it contains a number of elements with decay half-lives on the order of hours and days. The database showed that the U1a soil was made of 18 different oxides, with 6.48% of the total sample lost on ignition (LOI), and accounting for a total of (98.57 ± 1)% of the U1a rock sample. The abundance of these 18 oxides was reported in ppm or percent of total. In calculating the soil composition, these relative measures were assumed to be on a mass basis. The LOI mass was assumed to be water. Oxides were assumed to have perfect stoichiometry. The stoichiometry of each oxide was used to compute its component isotopic weight fractions, and these were multiplied by the reported oxide weight fraction to get the weight fraction of each oxide's components in the soil. The sum of all component weight fractions was normalized to unity. The grain density of the soil was estimated by multiplying the reported oxide weight fraction by its handbook density and summing over all 18 oxides (not water). Uniform sampling of the grain density, water fraction, and porosity were used to estimate the bulk density as 1.96 g/cm^3 ± 6%. See Ref. X.

(Note that all references to "tuff"[3,4] have been replaced with "soil.") "X" is a reference to this memo.

Acknowledgment

Garrett Euler (EES-17) pointed out the error in the density calculation of Ref. 2 and very patiently helped me correct it. He provided Refs. 14 and 15. He also noted that it is incorrect to refer to the U1a soil as "tuff."

References

1. Christopher J. Werner, ed., "MCNP® User's Manual, Code Version 6.2," Los Alamos National Laboratory report LA–UR–17–29981, Rev. 0 (Oct. 27, 2017).

2. Jeffrey A. Favorite, "(U) Recalculation of Soil Used in the Scorpius MCNP6 Model," Los Alamos National Laboratory report LA–UR–20–27105 (September 10, 2020).

3. Jordan J. Douglas, "60% Radiological Engineering Design Review of the Plug B Structure," June 2020, transmitted under cover letter RP-20-015, June 11, 2020.

4. MCNP input file SCORPIUS-Mark4-Model_CSG-FXR_Geo_Splitting.mcnp.i, email from Jordan J. Douglas, LANL RP-PROG, to Josh B. Spencer, LANL XCP-7, July 21, 2020.

5. "Mercury Core Library and Data Center," https://www.sciencebase.gov/mercury/#/, accessed Sept. 8, 2020.

6. "NNSS PGG Database," https://www.sciencebase.gov/mercury/#/data/pgg_database, accessed Sept. 8, 2020.

7. "nnss_pgg_db_180223," https://www.sciencebase.gov/catalog/file/get/58a31d38e4b0c82512869a9d?name=nnss_pgg_db.zip, accessed Sept. 8, 2020.

8. U.S. Department of the Interior, U.S. Geological Survey, "Digitally Available Interval-Specific Rock-Sample Data Compiled from Historical Records, Nevada National Security Site and Vicinity, Nye County, Nevada," Data Series 297, Version 2.2 (February 2017); https://pubs.usgs.gov/ds/2007/297/pdf/ds297.pdf.

9. NNSS_PGG_U1A_06212018.xlsx, email from J. Tim Goorley, LANL XCP-7, Sept. 3, 2020.

10. Email from Ed Kwicklis, LANL EES-16, Sept. 9, 2020.

11. Wim Haeck, LANL XCP-5, https://xcp-stash.lanl.gov/projects/FAUST/repos/elementary/browse, accessed Sept. 8, 2020.

12. K. J. R. Rosman and P. D. P. Taylor, "Isotopic Compositions of the Elements 1997," *Pure & Appl. Chem.*, **70**, *1*, 217–235 (1998); https://doi.org/10.1351/pac199870010217.

13. "Physical Constants of Inorganic Compounds," in CRC Handbook of Chemistry and Physics, 101st Edition, John R. Rumble, ed., CRC Press/Taylor & Francis, Boca Raton, FL (Internet Version 2020); http://hbcponline.com/faces/documents/04_02/04_02_0001.xhtml, accessed Sept. 8, 2020.

14. Brian M. Allen, "Preliminary Geologic Site Characterization of the LYNER Horizontal Drift Complex, Yucca Flat, Nevada Test Site," Raytheon Services Nevada report TSP:DGP:080:95 (May 1995).

15. Nancy W. Howard, "Variation in Properties of Nuclear Test Areas and Media at the Nevada Test Site," Lawrence Livermore National Laboratory report UCRL-53721, p. 21 (Sept. 15, 1985); https://llnl.primo.exlibrisgroup.com/discovery/delivery/01LLNL_INST:01LLNL_INST/1245360680006316?lang=en.

16. Jeffrey A. Favorite, "(U) Surface Source Calculated for 100 Drift," Los Alamos National Laboratory report LA–UR–21–20792 (Jan. 27, 2021).

JAF:jaf

Distribution:
J. T. Goorley, XCP-7, MS A143, `jgoorley@lanl.gov`
C. G. Rosaire IV, Mission Support and Test Services, `RosairCG@nv.doe.gov`
R. H. Lane, ASD-TECH, MS H816, `lanerh@lanl.gov`
J. R. Curtis, RP-PROG, MS K788, `jcurtis@lanl.gov`
J. J. Douglas, RP-PROG, MS K788, `jdouglas@lanl.gov`
G. G. Euler, EES-17, MS F665, `ggeuler@lanl.gov`
J. L. Alwin, XCP-7, MS A143, `jalwin@lanl.gov`
J. D. Court, XCP-7, MS A143, `davec@lanl.gov`
T. C. McClanahan, XCP-7, MS A143, `tcmcclan@lanl.gov`
J. B. Spencer, XCP-7, MS A143, `jspencer@lanl.gov`
J. A. Favorite, XCP-7, MS F663, `fave@lanl.gov`
National Security Research Center, `nsrc-cataloging@lanl.gov`
XCP-7 File

Appendix A
File Listings for Composition Calculation (Sec. III)

Elementary Input

```
# run with "python3 <file>"
import sys
sys.path.append( '/yellow/users/fave/faust' )
from elementary.Element import Element
from elementary.Nuclide import Nuclide
from elementary.AbundanceTable import AbundanceTable

table = AbundanceTable.default()

composition = table.decompose( Element( 13 ), 2. )
print (composition)
composition = table.decompose( Element(  8 ), 3. )
print (composition)

composition = table.decompose( Element( 56 ), 1. )
print (composition)
composition = table.decompose( Element(  8 ), 1. )
print (composition)

composition = table.decompose( Element( 20 ), 1. )
print (composition)
composition = table.decompose( Element(  8 ), 1. )
print (composition)

composition = table.decompose( Element( 26 ), 2. )
print (composition)
composition = table.decompose( Element(  8 ), 3. )
print (composition)

composition = table.decompose( Element( 19 ), 2. )
print (composition)
composition = table.decompose( Element(  8 ), 1. )
print (composition)

composition = table.decompose( Element( 12 ), 1. )
print (composition)
composition = table.decompose( Element(  8 ), 1. )
print (composition)

composition = table.decompose( Element( 25 ), 1. )
print (composition)
composition = table.decompose( Element(  8 ), 1. )
print (composition)

composition = table.decompose( Element( 11 ), 2. )
print (composition)
composition = table.decompose( Element(  8 ), 1. )
print (composition)

composition = table.decompose( Element( 41 ), 2. )
print (composition)
composition = table.decompose( Element(  8 ), 5. )
print (composition)

composition = table.decompose( Element( 28 ), 1. )
print (composition)
composition = table.decompose( Element(  8 ), 1. )
print (composition)

composition = table.decompose( Element( 15 ), 2. )
print (composition)
composition = table.decompose( Element(  8 ), 5. )
print (composition)

composition = table.decompose( Element( 37 ), 2. )
print (composition)
```

```
composition = table.decompose( Element(  8 ), 1. )
print (composition)

composition = table.decompose( Element( 14 ), 1. )
print (composition)
composition = table.decompose( Element(  8 ), 2. )
print (composition)

composition = table.decompose( Element( 38 ), 1. )
print (composition)
composition = table.decompose( Element(  8 ), 1. )
print (composition)

composition = table.decompose( Element( 22 ), 1. )
print (composition)
composition = table.decompose( Element(  8 ), 2. )
print (composition)

composition = table.decompose( Element( 39 ), 2. )
print (composition)
composition = table.decompose( Element(  8 ), 3. )
print (composition)

composition = table.decompose( Element( 30 ), 1. )
print (composition)
composition = table.decompose( Element(  8 ), 1. )
print (composition)

composition = table.decompose( Element( 40 ), 1. )
print (composition)
composition = table.decompose( Element(  8 ), 2. )
print (composition)

composition = table.decompose( Element(  1 ), 2. )
print (composition)
composition = table.decompose( Element(  8 ), 1. )
print (composition)

# these two were not detected
composition = table.decompose( Element( 24 ), 2. )
print (composition)
composition = table.decompose( Element(  8 ), 3. )
print (composition)

composition = table.decompose( Element( 23 ), 2. )
print (composition)
composition = table.decompose( Element(  8 ), 3. )
print (composition)
```

Elementary Output

```
{Al27: 2.0}
{O16: 2.9927099999999998, O17: 0.00114, O18: 0.006150000000000001}
{Ba130: 0.00106, Ba132: 0.00101, Ba134: 0.02417, Ba135: 0.06592, Ba136: 0.07854, Ba137: 0.11232, Ba138:
0.71698}
{O16: 0.99757, O17: 0.00038, O18: 0.00205}
{Ca40: 0.96941, Ca42: 0.00647, Ca43: 0.00135, Ca44: 0.02086, Ca46: 4e-05, Ca48: 0.00187}
{O16: 0.99757, O17: 0.00038, O18: 0.00205}
{Fe54: 0.1169, Fe56: 1.83508, Fe57: 0.04238, Fe58: 0.00564}
{O16: 2.9927099999999998, O17: 0.00114, O18: 0.006150000000000001}
{K39: 1.865162, K40: 0.000234, K41: 0.134604}
{O16: 0.99757, O17: 0.00038, O18: 0.00205}
{Mg24: 0.7899, Mg25: 0.1, Mg26: 0.1101}
{O16: 0.99757, O17: 0.00038, O18: 0.00205}
{Mn55: 1.0}
{O16: 0.99757, O17: 0.00038, O18: 0.00205}
{Na23: 2.0}
{O16: 0.99757, O17: 0.00038, O18: 0.00205}
{Nb93: 2.0}
{O16: 4.98785, O17: 0.0019000000000000002, O18: 0.01025}
{Ni58: 0.680769, Ni60: 0.262231, Ni61: 0.011399, Ni62: 0.036345, Ni64: 0.009256}
{O16: 0.99757, O17: 0.00038, O18: 0.00205}
```

```
{P31: 2.0}
{O16: 4.98785, O17: 0.0019000000000000002, O18: 0.01025}
{Rb85: 1.4434, Rb87: 0.5566}
{O16: 0.99757, O17: 0.00038, O18: 0.00205}
{Si28: 0.922297, Si29: 0.046832, Si30: 0.030872}
{O16: 1.99514, O17: 0.00076, O18: 0.0041}
{Sr84: 0.0056, Sr86: 0.0986, Sr87: 0.07, Sr88: 0.8258}
{O16: 0.99757, O17: 0.00038, O18: 0.00205}
{Ti46: 0.0825, Ti47: 0.0744, Ti48: 0.7372, Ti49: 0.0541, Ti50: 0.0518}
{O16: 1.99514, O17: 0.00076, O18: 0.0041}
{Y89: 2.0}
{O16: 2.9927099999999998, O17: 0.00114, O18: 0.006150000000000001}
{Zn64: 0.4863, Zn66: 0.279, Zn67: 0.041, Zn68: 0.1875, Zn70: 0.0062}
{O16: 0.99757, O17: 0.00038, O18: 0.00205}
{Zr90: 0.5145, Zr91: 0.1122, Zr92: 0.1715, Zr94: 0.1738, Zr96: 0.028}
{O16: 1.99514, O17: 0.00076, O18: 0.0041}
{H1: 1.99977, H2: 0.00023}
{O16: 0.99757, O17: 0.00038, O18: 0.00205}
{Cr50: 0.0869, Cr52: 1.67578, Cr53: 0.19002, Cr54: 0.0473}
{O16: 2.9927099999999998, O17: 0.00114, O18: 0.006150000000000001}
{V50: 0.005, V51: 1.995}
{O16: 2.9927099999999998, O17: 0.00114, O18: 0.006150000000000001}
```

MCNP6.2 Input File

```
soil material
 1   1  1.   -1     imp:n=1
 2   2  1.   -2  1  imp:n=1
 3   3  1.   -3  2  imp:n=1
 4   4  1.   -4  3  imp:n=1
 5   5  1.   -5  4  imp:n=1
 6   6  1.   -6  5  imp:n=1
 7   7  1.   -7  6  imp:n=1
 8   8  1.   -8  7  imp:n=1
 9   9  1.   -9  8  imp:n=1
10  10  1.  -10  9  imp:n=1
11  11  1.  -11 10  imp:n=1
12  12  1.  -12 11  imp:n=1
13  13  1.  -13 12  imp:n=1
14  14  1.  -14 13  imp:n=1
15  15  1.  -15 14  imp:n=1
16  16  1.  -16 15  imp:n=1
17  17  1.  -17 16  imp:n=1
18  18  1.  -18 17  imp:n=1
19  19  1.  -19 18  imp:n=1
20  20  1.  -20 19  imp:n=1
21  21  1.  -21 20  imp:n=1
99   0          21  imp:n=0

 1   so    1.
 2   so    2.
 3   so    3.
 4   so    4.
 5   so    5.
 6   so    6.
 7   so    7.
 8   so    8.
 9   so    9.
10   so   10.
11   so   11.
12   so   12.
13   so   13.
14   so   14.
15   so   15.
16   so   16.
17   so   17.
18   so   18.
19   so   19.
20   so   20.
21   so   21.

mode n
```

```
sdef
m01   13027  2.0
      8016  2.9927099999999998  8017  0.00114  8018  0.006150000000000001
m02   56130  0.00106  56132  0.00101  56134  0.02417  56135  0.06592
      56136  0.07854  56137  0.11232  56138  0.71698
      8016  0.99757  8017  0.00038  8018  0.00205
m03   20040  0.96941  20042  0.00647  20043  0.00135  20044  0.02086
      20046  4e-05  20048  0.00187
      8016  0.99757  8017  0.00038  8018  0.00205
m04   26054  0.1169  26056  1.83508  26057  0.04238  26058  0.00564
      8016  2.9927099999999998  8017  0.00114  8018  0.006150000000000001
m05   19039  1.865162  19040  0.000234  19041  0.134604
      8016  0.99757  8017  0.00038  8018  0.00205
m06   12024  0.7899  12025  0.1  12026  0.1101
      8016  0.99757  8017  0.00038  8018  0.00205
m07   25055  1.0
      8016  0.99757  8017  0.00038  8018  0.00205
m08   11023  2.0
      8016  0.99757  8017  0.00038  8018  0.00205
m09   41093  2.0
      8016  4.98785  8017  0.0019000000000000002  8018  0.01025
m10   28058  0.680769  28060  0.262231  28061  0.011399  28062  0.036345  28064  0.009256
      8016  0.99757  8017  0.00038  8018  0.00205
m11   15031  2.0
      8016  4.98785  8017  0.0019000000000000002  8018  0.01025
m12   37085  1.4434  37087  0.5566
      8016  0.99757  8017  0.00038  8018  0.00205
m13   14028  0.922297  14029  0.046832  14030  0.030872
      8016  1.99514  8017  0.00076  8018  0.0041
m14   38084  0.0056  38086  0.0986  38087  0.07  38088  0.8258
      8016  0.99757  8017  0.00038  8018  0.00205
m15   22046  0.0825  22047  0.0744  22048  0.7372  22049  0.0541  22050  0.0518
      8016  1.99514  8017  0.00076  8018  0.0041
m16   39089  2.0
      8016  2.9927099999999998  8017  0.00114  8018  0.006150000000000001
m17   30064  0.4863  30066  0.279  30067  0.041  30068  0.1875  30070  0.0062
      8016  0.99757  8017  0.00038  8018  0.00205
m18   40090  0.5145  40091  0.1122  40092  0.1715  40094  0.1738  40096  0.028
      8016  1.99514  8017  0.00076  8018  0.0041
m19   1001  1.99977  1002  0.00023
      8016  0.99757  8017  0.00038  8018  0.00205
c these two were not detected
m20   24050  0.0869  24052  1.67578  24053  0.19002  24054  0.0473
      8016  2.9927099999999998  8017  0.00114  8018  0.006150000000000001
m21   23050  0.005  23051  1.995
      8016  2.9927099999999998  8017  0.00114  8018  0.006150000000000001
print
```

MCNP6.2 Output (Print Table 40)

```
1material
print table 40
  number     component nuclide, mass fraction

       1          13027, 5.29251E-01       8016, 4.69474E-01       8017, 1.90062E-04       8018,
1.08566E-03

       2          56130, 8.98089E-04      56132, 8.68893E-04      56134, 2.11084E-02      56135,
5.80004E-02
                  56136, 6.96159E-02      56137, 1.00291E-01      56138, 6.44869E-01       8016,
1.04066E-01
                   8017, 4.21302E-05       8018, 2.40652E-04
       3          20040, 6.90833E-01      20042, 4.84103E-03      20043, 1.03418E-03      20044,
1.63508E-02
                  20046, 3.27787E-05      20048, 1.59906E-03       8016, 2.84536E-01       8017,
1.15192E-04
                   8018, 6.57988E-04
       4          26054, 3.94865E-02      26056, 6.42783E-01      26057, 1.51102E-02      26058,
2.04613E-03
                   8016, 2.99759E-01       8017, 1.21355E-04       8018, 6.93192E-04
       5          19039, 7.71515E-01      19040, 9.92778E-05      19041, 5.85335E-02       8016,
1.69392E-01
```

```
                8017, 6.85769E-05      8018, 3.91718E-04
     6         12024, 4.70067E-01     12025, 6.19927E-02     12026, 7.09769E-02       8016,
3.95888E-01
                8017, 1.60272E-04      8018, 9.15489E-04
     7         25055, 7.74458E-01      8016, 2.24931E-01      8017, 9.10615E-05       8018,
5.20152E-04

     8         11023, 7.41857E-01      8016, 2.57443E-01      8017, 1.04224E-04       8018,
5.95336E-04

     9         41093, 6.99044E-01      8016, 3.00140E-01      8017, 1.21509E-04       8018,
6.94073E-04

    10         28058, 5.28038E-01     28060, 2.10405E-01     28061, 9.29880E-03      28062,
3.01339E-02
               28064, 7.92202E-03      8016, 2.13622E-01      8017, 8.64832E-05       8018,
4.94001E-04
    11         15031, 4.36421E-01      8016, 5.62052E-01      8017, 2.27542E-04       8018,
1.29974E-03

    12         37085, 6.55639E-01     37087, 2.58773E-01      8016, 8.53562E-02       8017,
3.45558E-05
                8018, 1.97386E-04
    13         14028, 4.29448E-01     14029, 2.25854E-02     14030, 1.54009E-02       8016,
5.31123E-01
                8017, 2.15021E-04      8018, 1.22822E-03
    14         38084, 4.53516E-03     38086, 8.17504E-02     38087, 5.87131E-02      38088,
7.00591E-01
                8016, 1.53992E-01      8017, 6.23424E-05      8018, 3.56106E-04
    15         22046, 4.74684E-02     22047, 4.37386E-02     22048, 4.42584E-01      22049,
3.31567E-02
               22050, 3.23937E-02      8016, 3.99573E-01      8017, 1.61764E-04       8018,
9.24010E-04
    16         39089, 7.87440E-01      8016, 2.11984E-01      8017, 8.58200E-05       8018,
4.90212E-04

    17         30064, 3.81949E-01     30066, 2.25977E-01     30067, 3.37123E-02      30068,
1.56470E-01
               30070, 5.32634E-03      8016, 1.96032E-01      8017, 7.93620E-05       8018,
4.53324E-04
    18         40090, 3.75386E-01     40091, 8.27740E-02     40092, 1.27913E-01      40094,
1.32451E-01
               40096, 2.17934E-02      8016, 2.58980E-01      8017, 1.04846E-04       8018,
5.98889E-04
    19          1001, 1.11873E-01      1002, 2.57139E-05      8016, 8.85695E-01       8017,
3.58566E-04
                8018, 2.04817E-03
    20         24050, 2.85565E-02     24052, 5.72673E-01     24053, 6.61869E-02      24054,
1.67860E-02
                8016, 3.14942E-01      8017, 1.27501E-04      8018, 7.28301E-04
    21         23050, 1.66623E-03     23051, 6.78092E-01      8016, 3.19374E-01       8017,
1.29296E-04
                8018, 7.38551E-04
```

Appendix B
File Listing for Soil Wall Thickness (Sec. V) and Soil Density Effect (Sec. VI) Calculations

This is the nominal case. The tunnel geometry and photonuclear physics options are all from the current Scorpius model,[4] as are the concrete and air material compositions and densities. The soil composition and density are from the main text of this report.

```
Soil wall thickness test
c Main Entry Drift
5415   3  -2.32    -5427                                  imp:n,p=4     imp:e=0 fcl:n,p=1. $Slab
5416   5  -1.96    -5428 5427 5429 5430                   imp:n,p=1     imp:e=0 fcl:n,p=1. $Silt
5916   4  -0.001205 (-5429:-5430)                         imp:n,p=1     imp:e=0 fcl:n,p=1.
9998   0            5428  -9999                           imp:n,p=1     imp:e=0
9999   0            9999                                  imp:n,p=0     imp:e=0

c Main Entry Drift
5427     RPP -149.52 -119.52 -182.8802 487.6798 -9479.28 -1339.85             $ Slab
5428     RPP -324.63 642.48 -335.2802 640.0798 -9479.28 -1339.85              $ Silt Outer Boundary
5429     REC  307.2 152.3998 -9479.28  0 0 8139.43 152.4 0 0 0 335.28 0       $ Tunnel Ceiling
5430     RPP -119.52 307.2 -182.8802 487.6798 -9479.28 -1339.85               $ Air
c
9999     RCC  165. 152. -9800.   0. 0. 9000.   10000.

mode p n
c -- Multithreading with Photonuclear --
dbcn 17j 2 52j 1
c
c Physics Options for MCNP611!
phys:p   50 $ EMCPF Lower energy threshold above which simple physics is used
          0 $ IDES  thick-target bremsstrhlung, 0=on
          0 $ NOCOH Thompson scattering, 0=on (default)
c Photonuclear reactions makes threading ineffective (warning message)
          1 $ ISPN  Photonuclear reactions, -1=analog, 0=off, 1=biased, @ each event
          0 $ NODOP Doppler energy broadening, 0=on
          j $ unused
          0 $ FISM  0=photofission from ACE, 1=photofission from LLNL fission model
c  ACE does not have photofission prompt gammas
c
phys:n  50  $ EMAX  Upper limit for neutron energy
         0  $ EMCNF > this #, implicit capture, < this # analog capture
         0  $ IUNR  0=unresolved resonance capture on (default)
        3j  $ unused
        0   $ COLIF Light ion recoil and NCIA control,Default=0 off
        0   $ CUTN  Table-based physics cutoffs (ie. Mix and Match)
        1   $ NGAM  Secondary photon production. 1=ACE (Default) 2=CGM
         J  $ unused
c
c Bias neutron production from photons
SPABI:n  p  20 10 $ For energies < 20 MeV, do 10 for 1 splitting
c
nps 1e7
prdmp j 1e6
sdef pos=0. 485.1398 -5409.57 vec=0. 1. 0. dir=1. erg=d1
si1 l 1. 2. 3. 4. 5. 6. 7. 8. 9. 10. 11. 12. 13. 14. 15.
sp1   1  1  1  1  1  1  1  1  1  1   1   1   1   1   1
rand gen=2 seed=110000001
print -30
fc001 total photon reflection
f001:p  5427.3
c001    0.  1.
fc011 photon reflection by source energy
f011:p  5427.3
c011    0.  1.
ft011   scx 1
fq011   u c
fc021 neutron reflection by source energy
f021:n  5427.3
c021    0.  1.
ft021   scx 1
fq021   u c
```

```
c Concrete
m3     1001  -2.210111E-02
       6012  -2.482180E-03
       8016  -5.748636E-01
       11023 -1.521066E-02
       12024 -9.865297E-04
       12025 -1.301042E-04
       12026 -1.489592E-04
       13027 -1.995626E-02
       14028 -2.798959E-01
       14029 -1.472695E-02
       14030 -1.005398E-02
       20040 -4.152464E-02
       20042 -2.909848E-04
       20043 -6.216277E-05
       20044 -9.828158E-04
       20046 -1.970268E-06
       20048 -9.611650E-05
       26054 -3.634351E-04
       26056 -5.916199E-03
       26057 -1.390746E-04
       26058 -1.883267E-05
mx3:p   0
        6012.70u
        8016.70u
       11023.70u
       12024.70u
       12025.70u
       12026.70u
       13027.70u
       14028.70u
       14029.70u
       14030.70u
       20040.70u
       20042.70u
       20043.70u
       20044.70u
       20046.70u
       20048.70u
       26054.70u
       26056.70u
       26057.70u
       26058.70u
c
c Air
m4    6012  -1.24000E-04
      7014  -7.55268E-01
      8016  -2.31781E-01
      18040 -1.28270E-02
mx4:p 6012.70u
      7014.70u
      8016.70u
      18040.70u
c
c J. A. Favorite, "(U) Recalculation of Soil Used in the Scorpius MCNP6 Model,"
c Los Alamos National Laboratory report LA-UR-20-27105, Sept. 10, 2020.
c new density 1.96 g/cm^3; documentation in progress.
m5     1001     -7.35469E-03   1002     -1.69047E-06
       8016     -5.08370E-01   8017     -2.05809E-04
       8018     -1.17560E-03
      11023     -1.51054E-02
      12024     -9.11348E-04  12025     -1.20189E-04
      12026     -1.37607E-04
      13027     -6.03520E-02
      14028     -2.96354E-01  14029     -1.55858E-02
      14030     -1.06279E-02
      15031     -6.23408E-05
      19039     -4.56954E-02  19040     -5.88004E-06
      19041     -3.46683E-03
      20040     -2.21124E-02  20042     -1.54953E-04
      20043     -3.31024E-05  20044     -5.23362E-04
      20046     -1.04919E-06  20048     -5.11833E-05
      22046     -5.76933E-05  22047     -5.31601E-05
      22048     -5.37918E-04  22049     -4.02988E-05
```

```
        22050     -3.93714E-05
        25055     -2.37834E-04
        26054     -5.41213E-04  26056     -8.81016E-03
        26057     -2.07104E-04  26058     -2.80448E-05
        28058     -4.43139E-06  28060     -1.76576E-06
        28061     -7.80371E-08  28062     -2.52889E-07
        28064     -6.64830E-08
        30064     -2.94072E-05  30066     -1.73985E-05
        30067     -2.59559E-06  30068     -1.20470E-05
        30070     -4.10088E-07
        37085     -1.23122E-04  37087     -4.85947E-05
        38084     -1.67800E-07  38086     -3.02475E-06
        38087     -2.17237E-06  38088     -2.59217E-05
        39089     -7.29297E-05
        40090     -8.65648E-05  40091     -1.90879E-05
        40092     -2.94970E-05  40094     -3.05435E-05
        40096     -5.02560E-06
        41093     -5.51686E-05
        56130     -4.69873E-07  56132     -4.54598E-07
        56134     -1.10437E-05  56135     -3.03453E-05
        56136     -3.64225E-05  56137     -5.24714E-05
        56138     -3.37390E-04
mx5:p     0         1002.70u
         8016.70u    8017.70u
         8018.70u
        11023.70u
        12024.70u   12025.70u
        12026.70u
        13027.70u
        14028.70u   14029.70u
        14030.70u
        15031.19u
        19039.19u               19040.19u
        19041.19u
        20040.70u   20042.70u
        20043.70u   20044.70u
        20046.70u   20048.70u
        22046.70u   22047.70u
        22048.70u   22049.70u
        22050.70u
        25055.70u
        26054.70u   26056.70u
        26057.70u   26058.70u
        28058.70u   28060.70u
        28061.70u   28062.70u
        28064.70u
        30064.70u   30066.70u
        30067.70u   30068.70u
        30070.70u
        37085.19u               37087.19u
        38084.70u   38086.70u
        38087.70u   38088.70u
        39089.19u
        40090.70u   40091.70u
        40092.70u   40094.70u
        40096.70u
        41093.70u
        56130.19u               56132.19u
        56134.19u               56135.19u
        56136.19u               56137.19u
        56138.19u
```